Relationship between the high-amplitude magnetic anomalies and serpentinized fore-arc mantle in the Cascadia subduction zone

Wen-Bin Doo (wenbindoo@gmail.com)
National Central University

Research Article

Keywords: magnetization-density ratio (MDR), low degree of serpentinization, reduction to the pole (RTP), IGRF

Posted Date: September 15th, 2021

DOI: https://doi.org/10.21203/rs.3.rs-888114/v1

Relationship between the high-amplitude magnetic anomalies and serpentinized fore-arc mantle in the Cascadia subduction zone

Wen-Bin Doo

Center for Environmental Studies, National Central University, Taiwan
Corresponding author. E-mail: wenbindoo@gmail.com (W.-B. D.)

A zone of significant high-amplitude magnetic anomalies is observed without a comparable gravity high along the Cascadia margin and is spatially correlated with the low-velocity fore-arc mantle wedge, which is understood to be serpentinized fore-arc mantle and is further considered to be the main source of the high-amplitude magnetic anomalies. To test this hypothesis, the magnetization-density ratio (MDR) is estimated along the Cascadia margin to highlight the physical characteristics of serpentinization (reduced density and increased magnetization). Interestingly, high MDR values are found only in central Oregon, where slab dehydration and fore-arc mantle serpentinization (50%-60% serpentinization) are inferred in conjunction with sparse seismicity. This result may indicate either poorly serpentinized fore-arc mantle (low degree of serpentinization) or that the fore-arc mantle is deeper than the Curie temperature isotherm for magnetite in northern and southern Cascadia. I thus propose that serpentinized fore-arc mantle may not be the major contributor to the high-amplitude magnetic anomalies in these segments. This finding means that magnetic anomaly highs and serpentinized fore-arc mantle may not be completely positively related in subduction zones. On the other hand, the MDR pattern reveals the segmentation of the Cascadia subduction zone, which is consistent with several previous observations.

Serpentinization of fore-arc mantle is a common feature that has been observed in many subduction zones worldwide and plays an important role in dynamic subduction processes[1-7]. In subduction zones, subducting oceanic crust generally contain free water[8-10]; as the temperature and pressure increase, large volumes of fluids are released, subsequently upwelling into and hydrating the overlying mantle producing serpentine minerals[4,11,12]. The major physical characteristics of serpentinization are its ability to reduce velocities and densities, as well as to increase the intensity of magnetization[4,13-15]. The serpentinite in the fore-arc is thus often characterized by very high magnetic susceptibility simultaneously with low density, which can result in relatively high magnetic and low gravity anomalies. Ref.[16] therefore suggested that magnetic data could be a useful tool for mapping serpentinized fore-arc mantle in subduction zones worldwide.

The Juan de Fuca plate is subducting obliquely northeastward beneath North America at a rate that ranges from 33 mm/yr at the southern part of the subduction zone to 43 mm/yr at the north (Fig. 1; ref.[17]). In central Oregon, ref.[2] found very low seismic velocity structure beneath the fore-arc region from a shear-wave velocity profile (black dashed line shown in Fig. 1) and interpreted the anomalies as serpentinized fore-arc mantle. In addition, according to seismic observations, ref.[3] presented that weak or missing PmP North American plate reflections and low upper-mantle velocities mark a narrow zone along the Cascadia margin from southern British to northern California. They further proposed that serpentinization of the fore-arc mantle is the most likely explanation for their observations. Several seismological studies[1,18-23] have similarly reported that serpentinization of the fore-arc mantle associated with slab dehydration is widespread along the Cascadia margin.

The global magnetic anomaly map[24] reveals a roughly continuous zone of significant high-amplitude magnetic anomalies along the Cascadia subduction zone

from 48.5°N to 43.5°N (Fig. 2). The cause of this prominent magnetic anomaly high has been interpreted as (1) Miocene granodiorite intrusions in western Cascadia[25], (2) accreted basalt basement in the fore-arc region[26], or (3) serpentinization of the fore-arc mantle[16]. To delineate the locations of the relevant magnetic sources, I deskewed the orientation of the magnetic sources by applying the reduction to the pole (RTP) method. The magnetization direction is presumed to be aligned with the present-day geomagnetic field, and the inclination and declination are set to 67.59° and 16.26°, respectively, in the study area (based on the International Geomagnetic Reference Field (IGRF) 11 model). Even though the inclination and declination vary over the study area. Using a single vector direction will not affect the conclusion. The deskewed magnetic anomaly is shown in Fig. 3a. Interestingly, this highly magnetic region has no comparable Bouguer gravity high[27] (Fig. 3b). In addition, the 2-D thermal model[28] indicates that the temperature of the mantle wedge in many subduction zones is lower than the Curie temperature of magnetite. Summarizing all this information, ref.[16] proposed that these high-amplitude magnetic anomalies could be caused by serpentinized fore-arc mantle, which seems feasible and reliable. To test this hypothesis, a combined magnetic and gravity data analysis method leveraging the magnetization-density ratio (MDR) was used in this study. The advantage of using the MDR is that it can strongly highlight the characteristics of serpentinization. Accordingly (if this hypothesis were 100% applicable), I expect to obtain obvious high MDR values along the entire Cascadia margin.

Segmentation of the Cascadia subduction zone

The Cascadia margin is a convergent plate boundary where a relatively young (< 15 Ma), warm, and thin plate is subducting beneath North America (Fig. 1). Notably, the entire subduction zone, including the subducting and overriding plates, is segmented

north to south, revealing lateral variations in several geophysical and geological characteristics. The subducting plate consists of the main Juan de Fuca plate and smaller plates to the north and south: the Explorer and Gorda plates, respectively. In the overriding plate, the along-strike topography of the fore-arc region can be divided roughly into the Washington, Oregon, and Sierra Nevada segments from north to south, with flat and low-lying topography in the center and higher elevations to the north and south[29]. In addition, the subducting slab and overriding North American crust appear roughly segmented into three parts according to the results of ambient noise tomography[29]. Variations in the distribution of seismicity also reflect this segmentation: seismicity occurs mainly in the northern and southern segments of the Cascadia subduction zone and sparsely in the central part[30]. On the other hand, the non-volcanic tremor density reveals similar features[23,31] (much higher in the northern and southern segments along the Cascadia margin). Overall, northern and southern Cascadia exhibits roughly similar geophysical and geological features, but central Cascadia exhibits different characteristics. Although no great earthquakes ($M > 8$) have been detected instrumentally along the Cascadia margin[32] and even though the structural characteristics are segmented, the length of the subduction zone (approximately 1100 km) is sufficient to generate magnitude 9 earthquakes[33], and the seismogenic zone is considered to be fully locked[34]. According to an analysis of marine turbidities, the recurrence interval of large earthquakes in the Cascadia margin is approximately 500 years[33], and the most recent great megathrust earthquake (M 9) occurred in 1700[35]. Considering the time span between this event and the present day, it is essential to better understand the background tectonic characteristics, which could be beneficial for hazard assessment and risk mitigation.

Magnetization-density ratio (MDR) results

Gravity and magnetic data can provide basic information on Earth's structures, but these data are usually processed and interpreted separately. The Poisson theorem provides a simple relationship between gravity and magnetic data such that they can be interpreted together[36-40]. Based on the Poisson theorem and the characteristics of analytic signal[41,42], ref.[40] provided a convenient method to calculate the MDR of subsurface materials directly using magnetic and gravity anomalies. Using this method, I do not need to obtain the magnetization and density of the subsurface materials individually. Thus, the MDR value is useful and convenient for establishing geophysical and geological interpretations. The serpentinization of mantle peridotite increases the intensity of magnetization and reduces the density[4,43]. Therefore, in general, if the high-amplitude magnetic anomalies along the onshore part of the Cascadia subduction zone (Fig. 2b) are the result of a serpentinized mantle wedge, the high and obvious MDR values should theoretically exhibit along the Cascadia margin.

Firstly, I estimate the zero-order analytic signal of the magnetic anomaly and the first-order analytic signal of the Bouguer gravity anomaly, separately. Then, the MDR values of the study area are determined. The result is shown in Fig. 4. The most obvious high MDR values are distributed in the central Cascadia fore-arc region.

Discussion

Relationship between the high-amplitude magnetic anomalies and serpentinized fore-arc mantle. Ref.[2] identified a highly serpentinized fore-arc upper mantle beneath central Oregon from a dense array of broadband seismometers. On the basis of their thermal modeling results, they pointed out that the fore-arc upper mantle beneath this region is colder than the typical continental upper mantle. Along the same profile, I obtained obvious high MDR values immediately above the serpentinized fore-arc mantle (Fig. 5). According to the characteristics of serpentinization, the MDR value

should increase dramatically with an increasing degree of serpentinization. Consequently, the very high MDR values in the central Cascadia fore-arc region (Fig. 4) are consistent with the observations of ref. 2 (high degree of serpentinization and low temperature), which may indicate that the serpentinized fore-arc mantle is responsible for the majority of the high-amplitude magnetic anomalies in this region. In contrast, the low MDR values in Washington seem inconsistent with the initial concept of serpentinization; in other words, the high-amplitude magnetic anomalies observed in this segment may not originate primarily from serpentinized fore-arc mantle. I therefore interpreted that high-amplitude magnetic anomalies and serpentinized fore-arc mantle may not be completely positively related in subduction zones.

Ref.[3] proposed that the fore-arc mantle along the entire Cascadia margin is serpentinized according to the seismic and the results of earthquake tomography. However, as shown in Fig. 4, high MDR values were distributed only in central Oregon. Based on Fig. 5, these high MDR values may delineate the region with serpentinized fore-arc mantle, similar to the feature proposed by ref.[2]. The degree of serpentinization of the fore-arc mantle, which is closely associated with the slab dehydration, could be a major factor for this segmented MDR pattern (Fig. 4). For example, ref.[44] proposed that the degree of serpentinization of the fore-arc mantle in the Kyushu subduction zone is strongly heterogeneous, varying from 0% to 12%. A similar feature has been reported along the strike of the Cascadia subduction zone, where the degree of serpentinization varies. Ref.[1] interpreted 15%-20% serpentinization of the upper mantle beneath the northern Cascadia subduction zone, and an upper mantle P-wave velocity of 7.6 km/s was obtained in Washington[45], which may indicate ~25% serpentinization[13], while ref.[2] proposed that the degree of serpentinization in central Oregon may be as high as 50%-60%. According to these

159 results, the degrees of serpentinization are higher in the central and low in the northern
160 and southern Cascadia. Ref.[30] similarly proposed that the degree of serpentinization is
161 heterogenous along the whole Cascadia fore-arc region. As mantle peridotite is
162 serpentinized from 0% to 95%, the magnetic susceptibility increases by several orders
163 of magnitude[43], and the degree of variation in the susceptibility is larger than that in
164 the density[43]. Hence, the degree of serpentinization may strongly affect the variations
165 in the MDR value and the observed magnetic anomalies. According to this
166 information, I propose the presence of a highly serpentinized (high degree of
167 serpentinization) mantle wedge beneath the central Cascadia fore-arc and its thermal
168 status is lower than the Curie-temperature of magnetite, whereas the low MDR values
169 present in the Cascadia margin may be due to a poorly serpentinized (low degree of
170 serpentinization) mantle wedge in those segments.

171 Another possibility is that the hydrated fore-arc mantle is deeper than the Curie
172 temperature isotherm; this would cause ferromagnetic materials to lose their
173 permanent magnetism in the northern and southern Cascadia margin. As mentioned
174 above, thermal modeling results[28] indicate that the mantle wedges in many subduction
175 zones are cooler than the Curie temperature of magnetite. However, the Cascadia
176 margin is warmer than other subduction zones. In addition, ref.[46] proposed that the
177 fore-arc mantle corner is shallow in Oregon (35-40 km) and deep beneath Washington
178 (41-43 km). These differences in depth may cause temperature differences reaching
179 several tens of degrees due to the geothermal gradient. Ref.[32] also proposed that the
180 temperature gradient changes from high in the north to low in the central region and
181 increases again in the southern Cascadia subduction zone. In summary, the thermal
182 state may also be a cause of the low MDR values found in the northern and southern
183 Cascadia margin. However, in this study, there is insufficient evidence to assert which
184 of these two factors is the major control.

Relationship between intraslab earthquake and serpentinized fore-arc mantle. Slab dehydration and eclogitization are believed to be mechanisms that produce intraslab earthquakes[11,12,16,30,47]. From this perspective, water released from a subducted slab could lead to brittle failure within the slab and hydration of the overlying mantle. Accordingly, the extent of serpentinized fore-arc mantle should spatially correlate with the distribution of intraslab earthquakes. Ref.[16] further suggested that magnetic anomaly highs in subduction zones could also be spatially correlated with intraslab earthquakes. However, the seismicity in northern and southern Cascadia is clustered, while seismicity is lacking in the central segment (Fig. 4), where slab eclogitization and fore-arc mantle serpentinization have been inferred[2] and high MDR values have been presented herein. The high MDR values calculated in this study may delineate the region with a high degree of serpentinization proposed by ref.[2] and may further indicate that the volume of released water (the magnitude of slab dehydration) is larger in this segment than that in northern and southern Cascadia. In Fig. 4, the spatial correlation between the distribution of intraslab earthquakes and serpentinized fore-arc mantle seems to vary if I consider the information mentioned above (e.g. the similar features are observed in the southern Alaska subduction zone by ref.[16]). Consequently, the proposed slab dehydration mechanism seems insufficient to explain the occurrence of intraslab earthquakes in the Cascadia subduction zone.

Previous studies[7,34,48,49] have suggested that along-strike variations in the earthquake distributions in subduction zones may be attributable to several factors, including the thermal structure of the incoming plate, degree of slab dehydration, plate coupling state, curvature of the subducting slab, and subducting features (barriers or asperities remain controversial). To explain the distribution of seismicity in the Cascadia subduction zone, for instance, ref.[50] proposed that changes in plate stress

and/or plate geometry may be the cause of the paucity of earthquakes in Oregon. Alternatively, ref.[16] postulated that the highly serpentinized fore-arc mantle beneath Oregon reduces friction on the downgoing slab, thereby explaining the scarcity of earthquakes. Ref.[51] suggested that the subducting Juan de Fuca slab appears to bend at a slightly steeper angle in central Cascadia than in the northern and southern parts, whereas ref.[32] considered that the sparse seismicity in central Cascadia is attributed to an unusually warm segment of the subducting slab. Ref.[52] proposed that a highly hydrated oceanic lithosphere can significantly reduce its strength, which could reduce the seismicity in central Cascadia. Summarizing all of the above concepts, both the properties and the geometries of the subducting plate seem to play important roles in the different distribution densities of earthquakes and segmented features throughout the Cascadia subduction zone. The MDR distribution pattern also reflects this segmentation and correlates well with the distribution of seismicity (Fig. 4). These likely factors may be related. However, the actual mechanism affecting the distribution of seismicity in Cascadia remains an open question and require further investigation in the future.

Conclusions

I estimate the MDR along the Cascadia margin to investigate the relationship between high-amplitude magnetic anomalies and serpentinized fore-arc mantle. The high MDR values observed in the Cascadia margin reflect the significant characteristics of the serpentinized mantle wedge[4]. However, high MDR values are segmentally distributed in the fore-arc region rather than along the entire Cascadia margin: the MDR values are higher in the central region and low in the north and south. According to the MDR results (Fig. 4), I propose that the serpentinized mantle wedge contributes to the majority of the high-amplitude magnetic anomalies only in central Cascadia.

Serpentinized fore-arc mantle has been thought to be ubiquitous in subduction zones worldwide. However, this feature may not necessarily result in high-amplitude magnetic anomalies due to the degree of serpentinization and/or the background thermal status. In other words, high magnetic anomalies in subduction zones do not inevitably result from a serpentinized mantle wedge (or vice versa). In addition, several previous studies have proposed that slab dehydration and embrittlement reactions are mechanisms that produce intraslab earthquakes. However, several significant features, including high MDR values, high degrees of serpentinization fore-arc mantle[2], and corresponding rare intraslab earthquakes, have been observed in central Cascadia. Integrating all these observations and estimation results, I propose that the high-amplitude magnetic anomalies, the serpentinized fore-arc mantle, and the occurrence of intraslab earthquakes in subduction zones are not completely positively correlated.

References

1. Zhao, D. Wang, K. Rogers, G.C. & Peacock, S.M. Tomographic image of low P velocity anomalies above slab in northern Cascadia subduction zone. Earth Planets Space **53**, 285-293 (2001).
2. Bostock, M.G. Hyndman, R.D. Rondenay, S. & Peacock, S.M. An inverted continental Moho and serpentinization of the forearc mantle. Nature **147**, 536-538 (2002).
3. Brocher, T.M. Parsons, T. Tréhu, A.M. Snelson, C.M. & Fisher, M.A. Seismic evidence for widespread serpentinized forearc upper mantle along the Cascadia margin. Geology **31**, 267-270 (2003).
4. Hyndman, R.D. & Peacock, S.M. Serpentinization of the forearc mantle. Earth Planet. Sci. Lett. **212**, 417-432 (2003).
5. Xia, S. Zhao, D. & Qiu, X. 2008. Tomography evidence for the subducting oceanic crust and forearc mantle serpentinization under Kyushu, Japan. Tectonophysics **449**, 85-96 (2008).
6. Chou, H.-C. Kuo, B.-Y. Chiao, L.-Y. Zhao, D. & Hung, S.-H. Tomography of the westernmost Ryukyu subduction zone and the serpentinization of the fore-arc mantle. J. Geophys. Res. **114**, B12301 (2009).
7. Doo, W.-B. et al. Variations in mantle lithosphere buoyancy reveal seismogenic behavior in the Sunda-Andaman subduction zone. Geophys. J. Int. **220**, 1275-1283 (2020).
8. Ranero, C.R. Phipps Morgan, J. McIntosh, K. & Relchert, C. Bending-related faulting and mantle serpentinization at the Middle America trench. Nature **425**, 367-373 (2003).
9. Shillington, D.J. et al. Link between plate fabric, hydration and subduction zone seismicity in Alaska. Nat. Geosi. **8**, 961-964 (2015).
10. Fujie, G. et al. Controlling factor of incoming plate htdration at the north-western Pacific margin. Nat. Commun. **9**(1):3844 (2018).
11. Kirby, S. Engdahl, E.R. & Denlinger, R. Intermediate-depth intraslab earthquakes and arc volcanism as physical expressions of crustal and uppermost mantle metamorphism in subducting slabs, in Bebout, G.E., et al., eds., Subduction: Top to bottom. AGU Geophysical Monograph 96, 195-214 (1996).
12. Peacock, S.M. Wang, K. & McMahon, A.M. Thermal structure and metamorphism of subducting oceanic crust: Insight into Cascadia intraslab earthquakes, in Kirby, S., et al., eds., The Cascadia subduction zone and related subduction systems-Seismic structure, intraslab earthquakes and process, and earthquake hazards. U.S. Geological Survey Open-File Report 02-328, 17-24 (2002).
13. Christensen, N. Elasticity of ultrabasic rocks. J. Geophys. Res. 71, 5921-5931 (1966).
14. Christensen, N. Serpentinites, peridotites, and seismology. Int. Geol. Rev. **46**, 759-816 (2004).
15. Horen, H. Zamore, M. & Dubuisson, G. Seismic waves velocities and anisotropy in

serpentinized peridotites from Xigaze ophiolite: abundance of serpentine in slow spreading ridge. Geophys. Res. Lett. **23**, 9-12 (1996).
16. Blakely, R.J. Brocher, T.M. & Wells, R.E. Subduction-zone magnetic anomalies and implications for hydrated forearc mantle. Geology **33**, 445-448 (2005).
17. Wilson, D.S. Confidence intervals for motion and deformation of the Juan de Fuca plate. J. Geophys. Res. **98**, 16053-16071 (1993).
18. Van Wagoner, T.M. et al. Crustal structure and relocated earthquakes in the Puget Lowland, Washington, from high-resolution seismic tomography. J. Geophys. Res. **107**, B12, 2381(2002).
19. Nicholson, T. Bostock, M.G. & Cassidy, J.F. New constraints on subduction zone structure in northern Cascadia. Geophys. J. Int. **161**, 849-859 (2005).
20. Abers, G.A. et al. Imaging the source of Cascadia tremor and intermediate-depth earthquakes. Geology **37**, 1119-1122 (2009).
21. Audet, P. Bostock, M.G. Christensen, N.I. & Peacock, S.M. Seismic evidence for overpressured subducted oceanic crust and megathrust fault sealing. Nature **457**, 76-78 (2009).
22. Delorey, A.A. & Vidale, J.E. Basin shear-wave velocities beneath Seattle, Washington, from noise-correlation Rayleigh waves. Bull. Seismol. Soc. Am. **101**, 2162-2175 (2011).
23. Delph, J.R. Levander, A. & Niu, F. Fluid controls on the heterogenous seismic characteristic of the Cascadia margin. Geophys. Res. Lett. **45**, 11021-11029 (2018).
24. Maus, S., et al. 2009. EMAG2: A 2-arc min resolution Earth Magnetic Anomaly Grid compiled from satellite, airborne, and marine magnetic measurements. Geochem. Geophys. Geosyst. **10**, Q08005 (2009).
25. Finn, C. U.S. West Coast revisited: An aeromagnetic perspective. Comment. Geology **19**, 950-951 (1991).
26. Wells, R.E. Weaver, C.S. & Blakely, R.J. Fore-arc migration in Cascadia and its neotectonic significance. Geology **26**, 759-762 (1998).
27. Balmino, G. Vales, N. Bonvalot, S. & Briais, A. Spherical harmonic modeling to ultrahigh degree of Bouguer and isostatic anomalies. J. Geodesy **86**, 499-520 (2012).
28. Oleskevich, D.A. Hyndman, R.D. & Wang, K. The updip and downdip limits to great subduction earthquakes: Thermal and structural models of Cascadia, south Alaska, SW Japan, and Chile. J. Geophys. Res. **104**, 14965-14991 (1999).
29. Porritt, R.W. Allen, R.M. Boyarko, D.C. & Brudzinski, M.R. Investigation of Cascadia segmentation with ambient noise tomography. Earth Planet. Sci. Lett. **309**, 67-76 (2011).
30. Chen, C. Zhao, D. & Wu, S. Tomographic imaging of the Cascadia subduction zone: Constraints on the Juan de Fuca slab. Tectonophysics **647-648**, 7388 (2015).
31. Wells, R.E. Blakely, R.J. Wech, A.G. McCrory, P.A. & Michael, A. Cascadia subduction tremor muted by crustal faults. Geology **45**, 515-518 (2017).

32. Ji, Y. Yoshioka, S. & Banay, Y.A. Thermal state, slab metamorphism, and interface seismicity in the Cascadia subduction zone based on 3-D modeling. Geophys. Res. Lett. **44**, 9242-9252 (2017).
33. Goldfinger, C. et al. Turbidite event history—Methods and implications for Holocene paleoseismicity of the Cascadia subduction zone: U.S. Geological Survey Professional Paper, 1661–F, 170 p (2012).
34. Wang, K. & Tréhu, A.M. Some outstanding issues in the study of great megathrust earthquakes-the Cascadia example. J. Geodyn. **98**, 1-18 (2016).
35. Satake, K. Shimazaki, K. Tsuji, Y. & Ueda, K. Time and size of a great earthquake in Cascadia inferred from Japanese tsunami records of January 1700. Nature **379**, 246-249 (1996).
36. Garland, G.D. Combined analysis of gravity and magnetic anomalies. Geophysics **16**, 51-62 (1951).
37. Hildebrand, T.G. Magnetic terranes in the central United States determined from the interpretation of digital data, in W. J. Hinze, ed., The utility of gravity and anomaly maps, SEG, 248-266 (1985).
38. Chandler, V.W. & Malek, K.C. 1991. Moving-window Poisson analysis of gravity and magnetic data from the Penokean orogen, east-central Minnesota. Geophysics **56**, 123-132 (1991).
39. Mendonca, C.A. Automatic determination of the magnetization-density ratio and magnetization inclination from the joint interpretation of 2D gravity and magnetic anomalies. Geophysics **69**, 938-948 (2004).
40. Doo, W.-B. Hsu, S.-K. Tsai, C.-H. & Huang, Y.-S. Using analytic signal to determine magnetization/density ratios of geological structures. Geophys. J. Int. 179, 112-124 (2009).
41. Roest, W.R. Verhoef, J. & Pilkington, M. Magnetic interpretation using the 3D analytic signal. Geophysics **57**, 116-125 (1992).
42. Hsu, S.-K. Sibuet, J.-C. & Shyu, C.-T. High-resolution detection of geologic boundaries from potential-field anomalies: An enhanced analytic signal technique. Geophysics **61**, 373-386 (1996).
43. Saad, A.F. Magnetic properties of ultramafic rocks from Red Mountain, California. Geophysics **34**, 974-987 (1969).
44. Xia, S. Sun, J. & Huang, H. Degree of serpentinization in the forearc mantle wedge of Kyushu subduction zone: quantitative evaluations from seismic velocity. Mar. Geophys. Res. **36**, 101-112 (2014).
45. Miller, K.C. et al. Crustal structure along the west flank of the Cascades, western Washington. J. Geophys. Res. **102**, 17857-17873 (1997).
46. McCrory, P.A. Hyndman, R.D. & Blair, J.L. Relationship between the Cascadia fore-arc

mantle wedge, nonvolcanic tremor, and the downdip limit of seismogenic rupture. Geochem. Geophys. Geosyst. **15**, 1071-1095 (2014).
47. Preston, L.A. Creager, K.C. Crosson, R.S. Brocher, T.M. & Trehu, A.M. Intraslab earthquakes: dehydration of the Cascadia slab. Science **302**, 1197-1200 (2003).
48. Wagner, L.S. Beck, S. & Zandt, G. Upper mantle structure in the south central Chilean subduction zone (30° to 36°S). J. Geophys. Res. **110**, B01308 (2005).
49. Bilek, S.L. Seismicity along the South American subduction zone: review of large earthquakes, tsunamis, and subduction zone complexity. Tectonophysics **495**, 2-14 (2009).
50. Brocher, T.M. et al. Mapping the magathrust beneath the northern Gulf of Alaska using wide-angle seismic reflection/refraction profiles. J. Geophys. Res. **99**, 11663-11685 (1994).
51. McCrory, P.A. Blair, J.L. Waldhauser, F. & Oppenheimer, D.H. 2012. Juan de Fuca slab geometry and its relation to Wadati-Benioff zone seismicity. J. Geophys. Res. **117**, B09306 (2012).
52. Gao, H. 2018. Three-dimensional variations of the slab geometry correlate with earthquake distributions at the Cascadia subduction zone. Nat. Commun. **9**, 1204 (2018).

Acknowledgements

I thank Benjamin Fong Chao and Shu-Kun Hsu for helpful discussions and comments. This work was supported by Ministry of Science and Technology of Taiwan (Grant No.: MOST 110-2116-M-008-014). Most of the figures are generated using the GMT software.

Author contribution

W.B Doo analyzed the data and wrote the paper.

Additional Information

Competing interests: The author declares no competing interests.

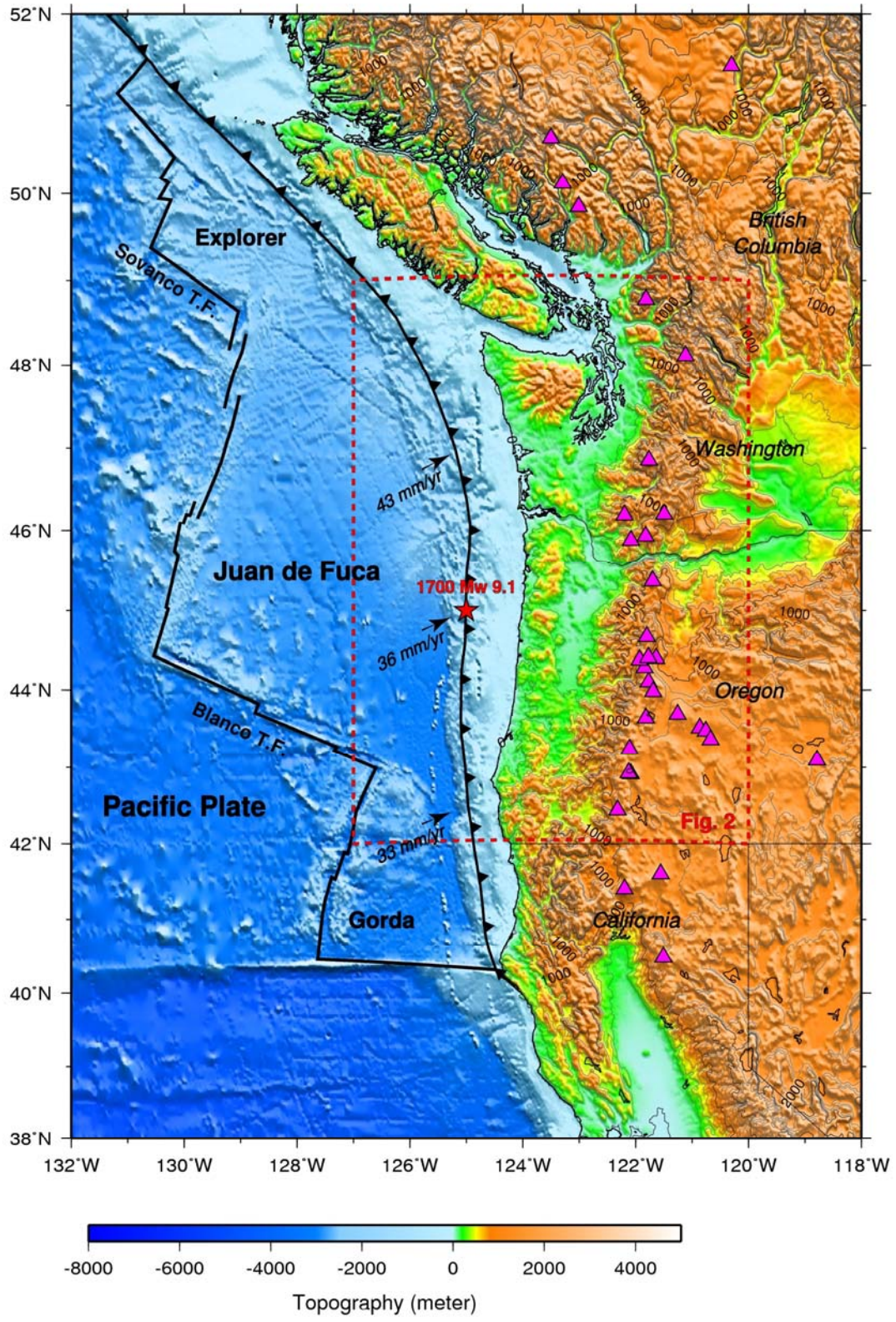

Figure 1. A regional map of the Cascadia subduction zone showing boundaries of tectonic plates. Black arrows illustrate the motion of the Juan de Fuca and Gorda plates with respect to the North American plate. Pink triangles denote active volcanoes of the Cascadia magmatic arc.

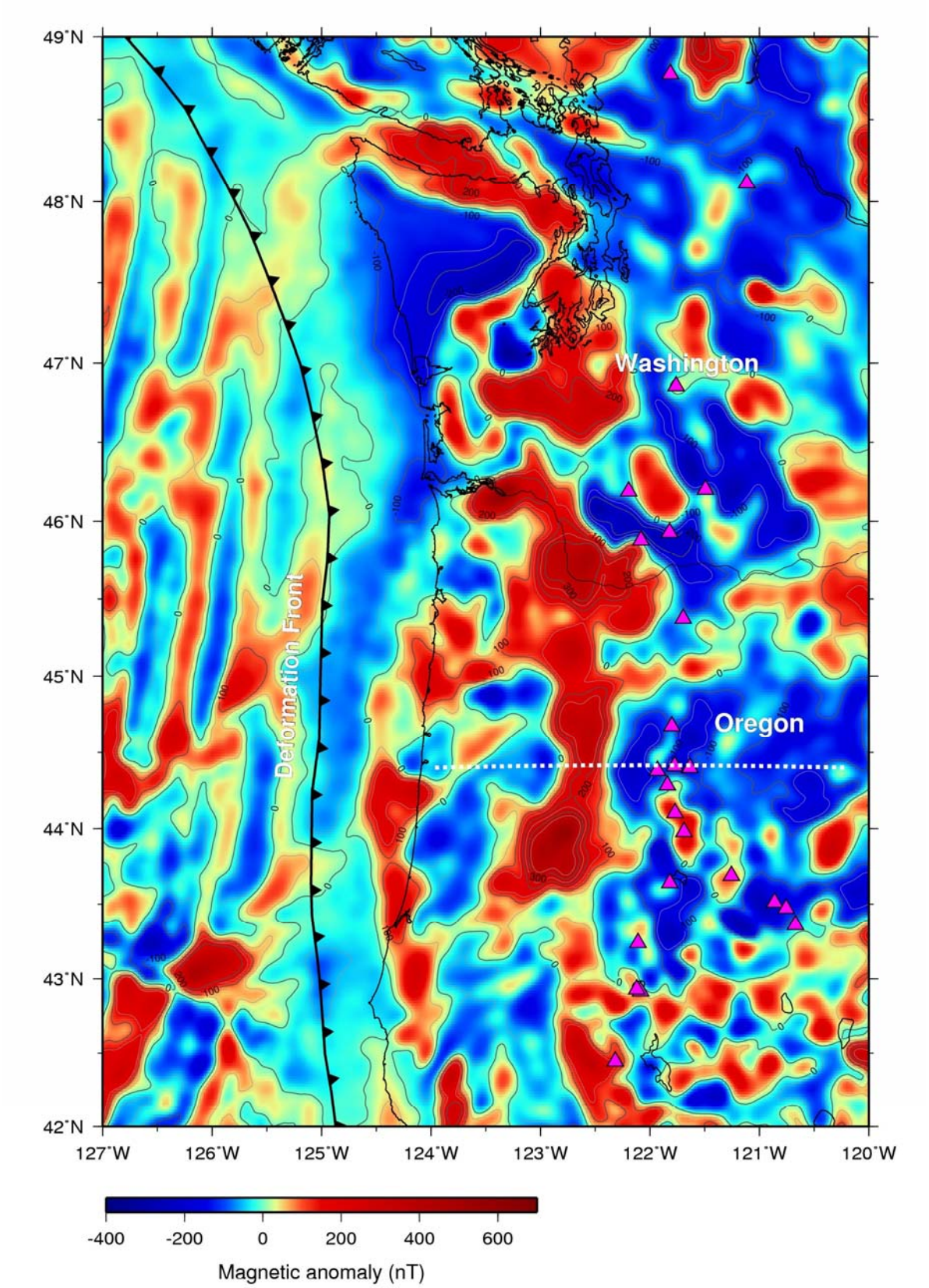

Figure 2. Magnetic anomaly map of the Cascadia margin[24]. Pink triangles denote active volcanoes of the Cascadia magmatic arc. White dashed line indicates the location of a shear-wave velocity model provided by ref. 2.

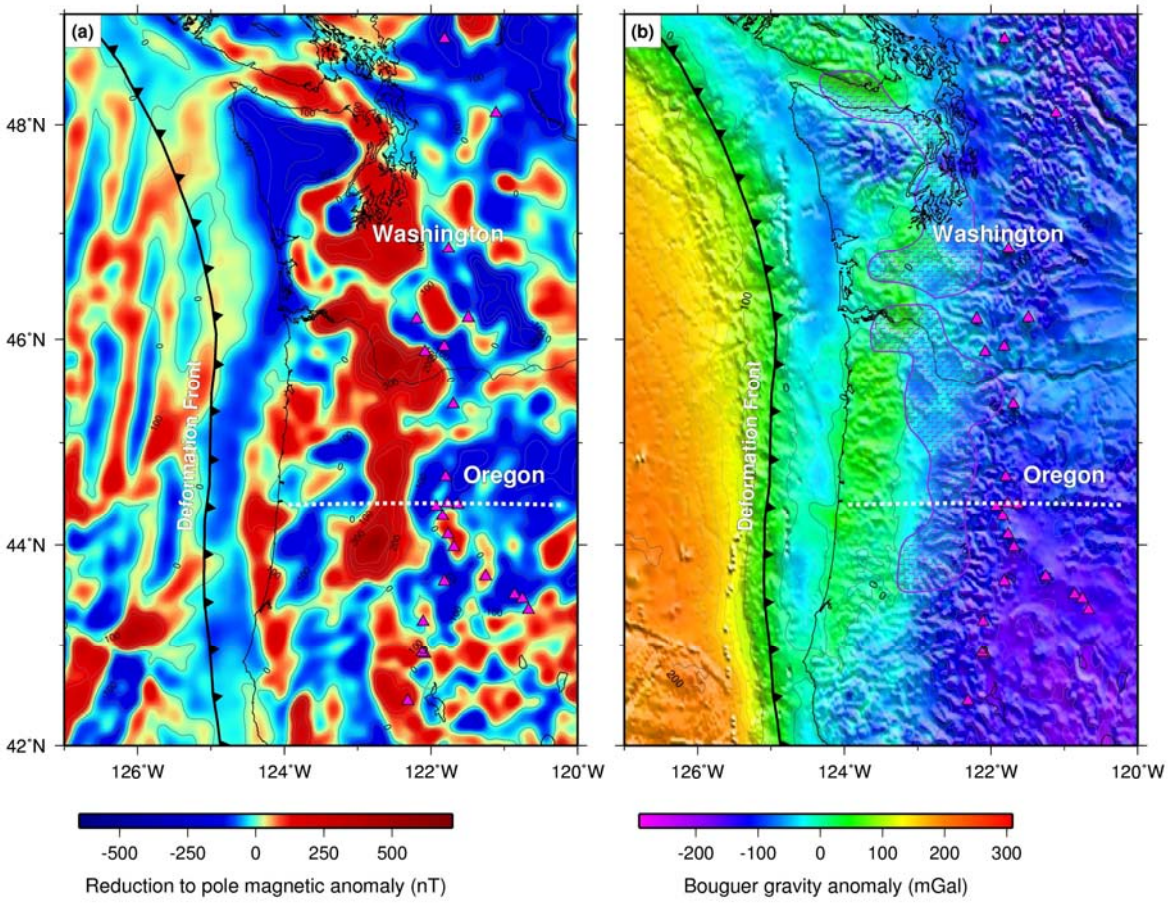

405

406 Figure 3. (a) Reduction to the pole magnetic anomaly map of the Cascadia margin. (b)
407 Bouguer gravity anomaly map of the Cascadia margin. Purple shadow pattern shows location
408 of magnetic anomalies of high amplitude. Pink triangles denote volcanoes. White dashed line
409 indicates the location of a shear-wave velocity model provided by ref. 2.

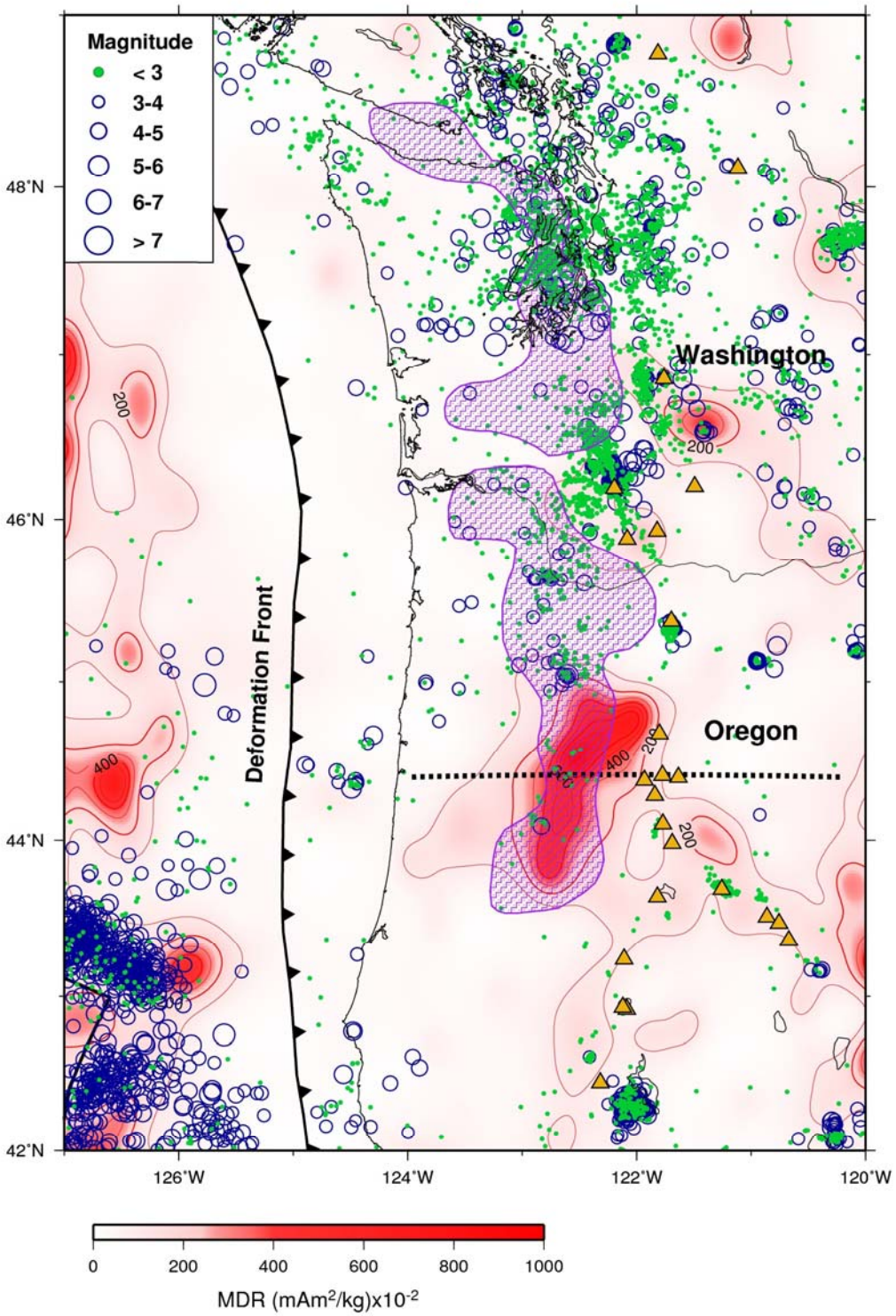

Figure 4. Magnetization – density ratio (MDR) values distribution map of the Cascadia margin. Black dashed line indicates the location of a shear-wave velocity model provided by ref. 2. Purple shadow pattern shows location of magnetic anomalies of high amplitude. The triangles denote volcanoes. Earthquakes occurred between 1900 and 2019 (USGS database), the size of the spheres indicate the magnitude of the events.

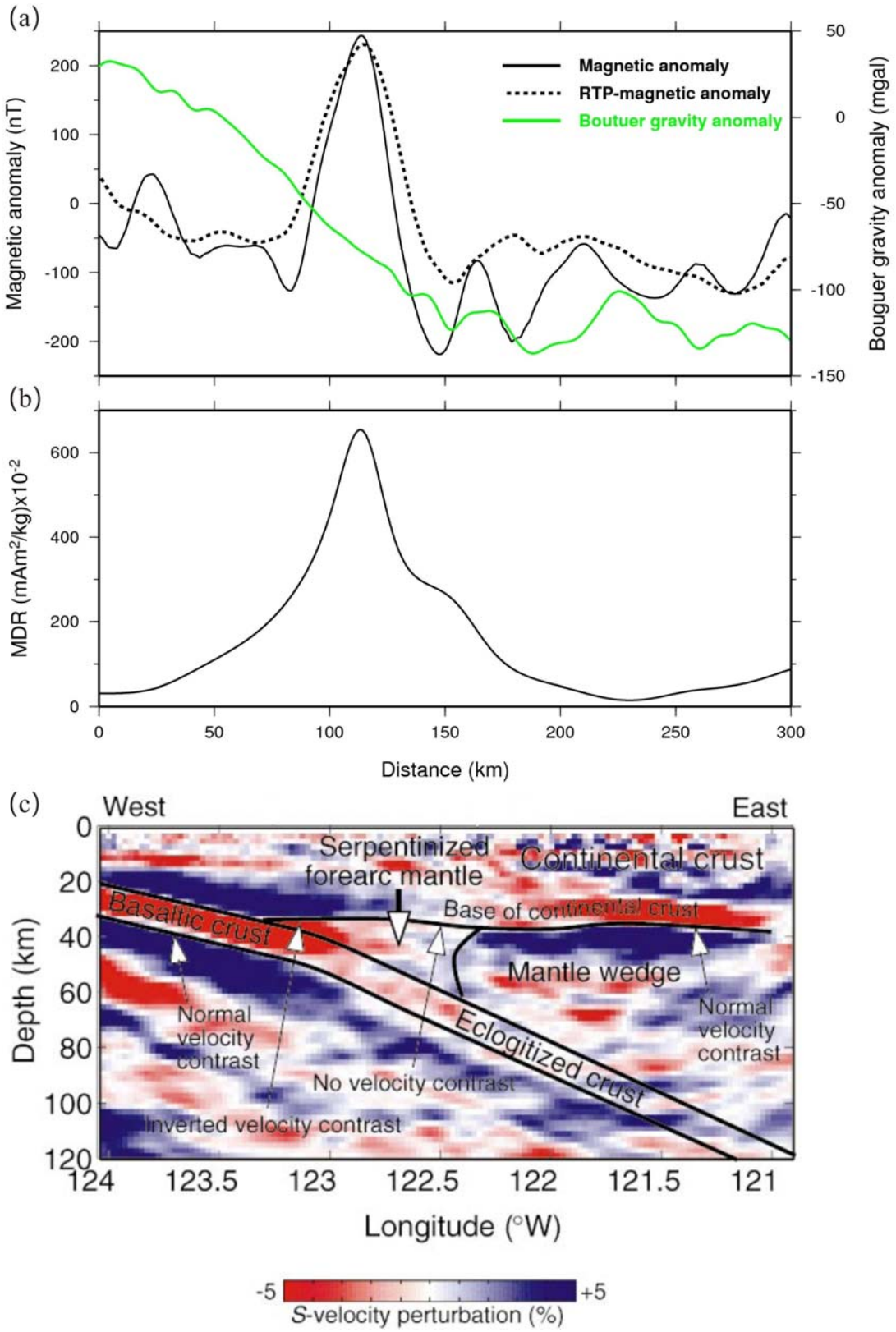

Figure 5. (a) Magnetic anomalies, both prior to and after reduction to the pole, and Bouguer gravity anomalies along the velocity profile of ref. 2 (profile location shown in Fig. 4); (b) MDR values along the velocity profile; (c) Interpreted shear-wave velocity model in central Oregon (identify from ref. 2,3).